

# 1    **Evaluating brain cell marker genes based on differential**

## 2    **gene expression and co-expression**

3    Rujia Dai<sup>1,4</sup>, Yu Chen<sup>1</sup>, Chuan Jiao<sup>1</sup>, Jiacheng Dai<sup>1</sup>, Chao Chen<sup>1,2\*</sup>, Chunyu Liu<sup>1,3,4\*</sup>

4

5    <sup>1</sup>Center for Medical Genetics, School of Life Sciences, Central South University, Changsha,  
6    China

7    <sup>2</sup>National Clinical Research Center for Geriatric Disorders, Xiangya Hospital, Central South  
8    University, Changsha, China

9    <sup>3</sup>School of Psychology, Shaanxi Normal University, Xi'an, China

10    <sup>4</sup>Department of Psychiatry, SUNY Upstate Medical University, Syracuse, NY, USA

11

## 12    **Abstract**

13    Reliable identification of brain cell types is necessary for studying brain cell  
14    biology. Many brain cell marker genes have been proposed, but their reliability  
15    has not been fully validated. We evaluated 540 commonly-used marker genes  
16    of astrocyte, microglia, neuron, and oligodendrocyte with six transcriptome and  
17    proteome datasets from purified human and mouse brain cells (n=125). By  
18    setting new criteria of cell-specific fold change, we identified 22 gold standard  
19    marker genes (GSM) with stable cell-specific expression. Our results call into  
20    question the specificity of many proposed marker genes. We used two single-  
21    cell transcriptome datasets from human and mouse brains to explore the co-  
22    expression of marker genes (n=3337). The mouse co-expression modules were  
23    perfectly preserved in human transcriptome, but the reverse was not. Also, we  
24    proposed new criteria for identifying marker genes based on both differential  
25    expression and co-expression data. We identified 16 novel candidate marker  
26    genes (NCM) for mouse and 18 for human independently, which have the  
27    potential for use in cell sorting or other tagging techniques. We validated the  
28    specificity of GSM and NCM by in-silico deconvolution analysis. Our systematic  
29    evaluation provides a list of credible marker genes to facilitate correct cell  
30    identification, cell labeling, and cell function studies.

31

## 32    **Introduction**

33    The human brain is a heterogeneous organ with numerous cell types. It has  
34    billions of cells including half neurons and half glia<sup>1</sup>. The major classes of glia  
35    are astrocyte, microglia and oligodendrocyte. Identifying these cell types is  
36    important because it would permit the brain to be understood in greater detail  
37    and would be especially useful for studying cellular contributions to the  
38    psychiatric disorders. A critical need in neuroscience research, is to develop  
39    methods to reliably identify specific brain cell types.

40    A strategy that has been employed to identify specific cell types is the

41 development of marker genes, which are sets of genes that express specifically  
42 in a cell type. Thousands of genes have been proposed as marker genes<sup>2</sup>. One  
43 well-known marker gene, RBFOX3 (gene of NeuN), is only expressed in nuclei  
44 of most neuronal cell types<sup>3</sup>. Marker genes can be used in several applications.  
45 Protein products of marker genes can be used to label different cell types, which  
46 may be used in fluorescence activated cell sorting (FACS). Marker genes also  
47 can be used to determine cell composition in bulk tissue samples. A  
48 computational method known as supervised deconvolution was developed to  
49 infer cell proportions in bulk tissue samples based on the expression of marker  
50 genes<sup>4-6</sup>. This method has been applied to studying the composition of bulk  
51 brain samples<sup>7,8</sup>. High specificity of marker genes is critical for generating  
52 reliable results in all of these applications.

53 Differential gene expression (DGE) analysis of transcriptome or proteome  
54 data is the most straightforward way to define the specificity of marker genes<sup>9-15</sup>. One of the drawbacks of DGE is that the outcomes is study-dependent. The  
55 outcomes are affected by many factors such as species, cell or tissue source,  
56 and the data generation platform. Human and mouse genomes are 80%  
57 orthologous<sup>16</sup>, but differences in gene expression between species are often  
58 greater than those between tissues within one species<sup>17</sup>. Within a species, cells  
59 isolated from primary culture or acutely from tissue showed different gene  
60 expression patterns<sup>18</sup>. Also, the expression estimates of the marker may vary  
61 considerably depending on whether mRNA or protein is measured. The  
62 statistical variation in transcriptome only explained 40% of the statistical  
63 variation in protein level<sup>19</sup>. Besides these biological confounders, the  
64 experimental platforms used to quantify gene expression level may also impact  
65 marker gene selection. RNA-Seq provides a larger dynamic range for the  
66 detection of transcripts and has less background noise, resulting in RNA-Seq  
67 being more sensitive in calling cell type-specific genes than microarray  
68 platforms<sup>20</sup>. Another weakness of DGE is that relationships among marker  
69 genes are not considered in the analysis. Groups of marker genes are often  
70 used to describe a cell type, and marker genes work with each other to execute  
71 functions in specific cell type. The relationship between marker genes  
72 represents their coordinated functions, specificities, and expressions. In DGE  
73 analysis, marker genes are defined independently, and the relationship among  
74 them is ignored.

75 Co-expression (COE) is a method of identifying interactions among genes by  
76 assigning genes with similar expression patterns into a module<sup>21,22</sup>. There was  
77 study reported that the co-expression modules in brain enriched cell type  
78 marker genes<sup>23</sup>. So it suggested that the co-expression can detected the cell  
79 type-specific marker genes, even in the heterogenous samples. The module  
80 formed by marker genes indicates their coordinated functions and specificities  
81 for a cell type. The correlation of genes with cell type-specific module suggests  
82 it's cell specificity. COE has the potential to systematically capture marker  
83 genes group that DGE cannot.

85 In this study, we evaluated the specificity of 540 published brain cell marker  
86 genes and discovered novel marker genes by DGE and COE analyses. We  
87 used six datasets containing transcriptome and proteome data from purified  
88 astrocytes, microglia, neurons and oligodendrocytes from both mouse and  
89 human brains. We identified 22 brain cell marker genes out of the 540  
90 candidates, referred as gold-standard marker genes (GSM), that specifically  
91 express in one cell type. We constructed brain cell-related gene co-expression  
92 modules for human and mouse, and found large differences among species.  
93 We found a statistically significant correlation between cell-specific fold change,  
94 a measure developed in this study, and gene membership in the brain cell-  
95 related coexpression modules. Combining DGE and COE, we identified 16  
96 novel candidate marker genes (NCM) in mouse brain and 18 NCM in the human  
97 brain. Through supervised cell deconvolution analysis, we showed that using  
98 GSM and NCM improved the performance of deconvolution.  
99

## 100 **Results**

101 To evaluate and discover brain cell marker genes, we performed DGE and  
102 COE analysis on transcriptomic or proteomic data (Figure 1). We used six  
103 datasets of purified cell populations for DGE analysis (DGEDat) and two single  
104 cell datasets for COE analysis (COEDat) (Table 1). The DGEDats included  
105 transcriptome and proteome data from human and mouse brain purified cell  
106 populations. The COEDats were single-cell RNA sequencing data from both  
107 human and mouse brains.

108

### 109 **Commonly-used marker genes of four major cell types**

110 We collected 540 marker genes that were commonly used for labeling cells  
111 and validating cell isolation (Supplementary Table 1). These marker genes were  
112 identified in published literature<sup>9,10,13-15</sup>, company websites<sup>24,25</sup>, and ISH  
113 databases, such as the Allen Brain Atlas (ABA) and GENSAT<sup>26-28</sup> for labeling  
114 neurons, astrocytes, microglia, oligodendrocytes, and other cell types in the  
115 brain. Of 540 candidate marker genes, only eight genes were reported in all  
116 data sources while most of the marker genes were source-specific  
117 (Supplementary Figure 1). Genes annotated as marker genes of more than two  
118 cell types by different sources were considered as “conflict marker genes.” We  
119 found 27 conflict marker genes in the 540 collected genes (Supplementary  
120 Table 1). The other genes had no conflict annotations in different data sources  
121 and were classified as “consistent marker genes.”

122

### 123 **DGE-based specificity evaluation of commonly-used marker genes**

124 We identified Gold-Standard Marker genes (GSM) that showed cell-type  
125 specificity across multiple types of data through DGE analysis. We found that  
126 the classical fold-change value, which is typically calculated as the expression  
127 in the target cell divided by averaged expression in other cells<sup>14,29</sup>, may produce

128 inaccurate calls of marker genes (Supplementary Figure 2, Supplementary  
129 Table 2). To avoid this problem, we created a measure of cell-specific fold  
130 change (csFC). The csFC was defined as equation (1).

131 
$$\text{csFC} = \frac{\text{expression in the target cell type}}{\text{the highest expression in all other cell types}} \quad (1)$$

132 To be considered a GSM, the following four criteria had to be met based the  
133 datasets we collected: 1) the gene must be detected in the target cell type in all  
134 six DGEDats. There were 113 of the 540 candidates that met this criterion. 2)  
135  $\text{csFC} \geq 2$  in all six DGEDats. 3) Benjamin-Hochberg (BH) corrected p-value of  
136 the two-sample Wilcoxon test of expression in the target cell, and expression in  
137 other cell types should be lower than 0.05 in more than two of the six DGEDats.  
138 4) the gene must be shown to be specific in at least one proteomic dataset.  
139 Using these criteria, we identified 22 GSM in total. Nineteen of the 22 GSM  
140 were from the consistent marker genes group, and three were from the conflict  
141 marker genes group (Table 2).

142

### 143 **COE analysis of two large single-cell datasets**

144 To discover the co-expression of marker genes, we performed weighted gene  
145 co-expression network analysis (WGCNA) on human and mouse brain single-  
146 cell transcriptome data in parallel with DGE. We annotated the co-expression  
147 modules using pSI packages<sup>30</sup>, which can identify genes enriched in specific  
148 cell populations and test gene overrepresentation by Fisher's exact test. Figure  
149 2A shows the p-value of cell type enrichment of each module after correcting  
150 for multiple testing by BH. We chose the most significant module in the cell type  
151 enrichment analysis as the brain cell co-expression module (BCCM) for each  
152 cell type (Table 3, Supplementary Figure 3 and Supplementary Figure 4). We  
153 used Gene Ontology analysis to determine the biological functions of each  
154 BCCM (Supplementary Table 3). The BCCMs were enriched in biological  
155 processes for specific cell types. For example, the oligodendrocyte-related  
156 module was enriched in the axon ensheathment pathway.

157 Next, we used the module preservation test to compare the BCCMs in  
158 human and mouse. The BCCMs of mouse brain were preserved in the human  
159 brain co-expression network. However, only the human neuron module was  
160 preserved in the mouse brain co-expression network (Figure 2B). Therefore,  
161 we analyzed the BCCMs for mouse and human brain separately in subsequent  
162 analysis to ensure we discover marker genes tailored specifically for human  
163 and mouse.

164

### 165 **DGE-COE relationship of brain cell marker genes**

166 After the independent analyses of DGE and COE, we explored the  
167 relationships between them. We first asked whether marker genes with stronger  
168 specificity have a higher probability to enter the BCCMs than those with lower  
169 specificity. We tested 107 marker genes covered by six DGEDats and human  
170 COEDat. These 107 genes had 72 clustered into the four cell-type specific

171 BCCMs and 35 into the other non-BCCMs. We found that csFC values of the  
172 72 BCCM marker genes were higher than those of the 35 non-BCCM marker  
173 genes in all six DGEDats (Figure 3A, p-value of two-sample Wilcoxon test  
174 <0.05). In other words, marker genes in the BCCMs were more specific than  
175 the marker genes in the non-BCCMs. Significantly higher csFC values of  
176 marker genes in BCCMs than in non-BCCMs were also observed in mouse  
177 data (Supplementary Figure 5A, p-value of two-sample Wilcoxon test <0.05).  
178 This suggests that the highly-specific marker genes are more likely to be placed  
179 in a BCCM.

180 Based on the test above, we next hypothesized that the highly-specific  
181 marker genes positioned close to the hub of the BCCMs have module  
182 membership rankings that are higher than non-GSM in the same BCCM. We  
183 divided the 72 marker genes in the human BCCMs into 20 GSM as identified  
184 above and 52 non-GSM. To compare the module membership ranking of these  
185 two gene groups, we performed a two-sample Wilcoxon test on their module  
186 membership (kME). kME is a measurement parameter used to assess the  
187 correlation between a gene and the eigengene, the hub of the co-expression  
188 module. A gene with high kME means that it has high correlations with other  
189 genes and consequently high ranking in the module. The kME values of GSM  
190 were significantly higher than those of non-GSM in the human BCCMs (p-value  
191 of two-sample Wilcoxon test <0.05, Figure 3B). However, the ranking of GSM in  
192 the BCCMs was not significantly higher than non-GSM in the mouse data (p-  
193 value of two-sample Wilcoxon test = 0.13, Supplementary Figure 5B).

194 These two analyses suggested that a connection did exist between DGE and  
195 COE for the marker genes. We further chose csFC representing DGE, and kME  
196 representing COE, to study the relationship between them. Significant  
197 correlations were observed between csFC values from five of the six DGEDats  
198 and kME values from human co-expression network (Spearman rho > 0.2, p <  
199 0.05; Figure 3C). In the mouse data, kME values of the marker genes were  
200 significantly correlated with csFC values in four of the six DGEDats (Spearman  
201 rho > 0.2, p < 0.05; Supplementary Figure 5C). This indicates that high cell-  
202 specific fold change and high correlation with other marker genes in the BCCMs  
203 are two related properties of marker genes.

204

## 205 **Novel candidate brain cell marker genes are revealed by integration of** 206 **COE and DGE**

207 Based on the relationship observed between DGE and COE, we developed  
208 new criteria for selecting novel candidate brain cell marker genes (NCM). Since  
209 the BCCMs of human and mouse were not completely preserved, NCM was  
210 defined in human and mouse separately. The mouse NCM should have 1) csFC  
211 equal to or greater than 2 in at least two DGEDats from DGEDat2-DGEDat6  
212 (BH corrected p-value of two samples of Wilcoxon test < 0.05), and 2) kME should  
213 be greater than 0.6 in COEDat2. We identified 16 mouse NCMs according to  
214 the criteria (Table 4, Supplementary Table S4). Because only one DGEDat for

215 the human brain was available for analysis, we set relatively stricter criteria for  
216 human NCM to make more conservative calls. The human NCM should have  
217 1) csFC significantly larger than 4 in the DGEDat1 (BH corrected p-value < 0.05)  
218 and 2) kME should be greater than 0.8 in the COEDat1. We identified 18 human  
219 NCM meeting these criteria (Table 4, Supplementary Table S5).

220

## 221 **GSM and NCM improve the performance of supervised deconvolution**

222 We used supervised deconvolution to examine how the choice of marker  
223 genes impacts deconvolution results using mouse data. We hypothesized that  
224 including GSM and NCM would improve deconvolution accuracy compared to  
225 not having them in the calculations. We downloaded mouse expression data  
226 from purified neuron, astrocyte, oligodendrocyte, and microglia, as well as RNA  
227 mixtures with known proportions of each cell type<sup>31</sup>. The purified cell expression  
228 data was used as a reference profile, and the mixture data was used for  
229 deconvolution. We constructed four types of reference gene sets: baseline,  
230 GSM\_plus, NCM\_plus, and NCM\_GSM\_plus. The baseline reference gene set  
231 included all the genes except for GSM and NCM. The other references were  
232 constructed by adding GSM, NCM, and their combination into the baseline  
233 reference. We used the root mean square error (RMSE) between estimated cell  
234 proportions and the true proportion to evaluate deconvolution performance.  
235 Higher RMSE indicated poorer performance of deconvolution. The optimal  
236 number of marker genes for deconvolution was determined (Materials and  
237 Methods). We found that the deconvolutions with baseline reference of 400  
238 genes had the lowest RMSE, so we used this number of genes to construct the  
239 four tested references.

240 We observed that adding either set of GSM or NCM into the reference  
241 reduced the RMSE (Figure 4), suggesting that the inclusion of GSM and NCM  
242 can improve the performance of deconvolution. The reference including both  
243 NCM and GSM performed the best. To prove that the improved performance of  
244 the reference with NCM or GSM was not because of a larger number of marker  
245 genes used, we completed permutations by constructing three permuted  
246 references with randomly selected genes, excluding GSM and NCM. The  
247 permutation was repeated 1000 times for each type of permuted reference.  
248 Deconvolution using a reference with GSM or NCM outperformed the  
249 deconvolution using a permuted reference without GSM or NCM, showing  
250 that improved deconvolution performance when GSM and NCM were included  
251 was not related to the increased reference size (Figure 4B).

252

## 253 **Discussion**

254 The current study describes the first systematic evaluation of marker gene  
255 specificity and their reliability for identifying cell types in human and mouse  
256 brains. We not only evaluated the published marker genes but also designed  
257 new criteria to discover novel marker genes based on both differential gene

258 expression and co-expression. Applying our proposed novel marker genes to  
259 deconvolution improved the performance of deconvolution and resulted in more  
260 accurate cell proportion estimates.

261 This study identified a set of marker genes to discriminate neurons,  
262 astrocytes, microglia, and oligodendrocytes. New brain cell types have recently  
263 been identified with the development of single-cell RNA sequencing<sup>32</sup>. The  
264 evaluation of marker genes for these new cell types cannot be achieved  
265 currently because the multi-omics for these new cell types are not available.  
266 We required the cell types in evaluation to be measured at both transcriptome  
267 and proteome level, and currently only the four major cell types above satisfied  
268 the criteria. Our method will be adaptable to the newly identified brain cell types  
269 when multi-omics data are available.

270 One of the important outcomes of the current study was validating the  
271 specificity of marker genes reported in the literature. Most of the genes  
272 (304/540) included in the current study were claimed to be marker genes in a  
273 single source, and only eight genes had a consistent claim supported by all the  
274 collection sources (Supplementary Figure 1). Some genes that we tested (27 /  
275 540) had conflict definitions for different cell types including several well-known  
276 marker genes, such as GFAP<sup>33</sup> and ITGAM<sup>34</sup>. Our evaluation refined a list of  
277 reliable marker genes and supported using GFAP as a marker of astrocytes  
278 and ITGAM as a marker of microglia.

279 We were strict in assessing the specificity of marker genes, which led to  
280 removing some genes from commonly used marker gene lists. We compared  
281 the classic fold-change and cell type-specific fold-change of consistent marker  
282 genes (Supplementary Table 2). Eight marker genes were imprecisely defined  
283 in more than three of six DGEDats using the classic fold change. For example,  
284 SELENBP1 was a claimed astrocyte marker gene using averaged ranks across  
285 comparisons with each of other cell types<sup>13</sup>. However, its expression in  
286 microglia is close to, or even higher than expression in astrocytes in DGEDat2-  
287 DGEDat6. We removed it from the marker gene list because of its similar  
288 expression in microglia and astrocyte (Supplementary Figure 2). Most of the  
289 candidate marker genes failed to meet our criteria of GSM due to either being  
290 expressed at a similar level in more than two cell types (17%) or not being  
291 detectable as protein in the target cell type (20%), such as RBFOX3 and  
292 TMEM119. These two genes both showed target cell specificity when they  
293 could be detected (Supplementary Table 6). We expect that more marker genes  
294 including these two genes may be reclassified as GSM when more reliable  
295 proteomics data becomes available.

296 We showed a positive correlation between the csFC and kME of marker  
297 genes in both human and mouse brain. This is in line with our expectation that  
298 good marker genes will have similar expression patterns across cell types and  
299 strongly correlate with each other, which forms the core part of the cell module.  
300 The most important meaning of the strong correlation is that it suggests COE  
301 can be used for discovering marker genes. COE used all cell types, both

302 characterized and uncharacterized, in brain tissue while DGE only used the  
303 several measured cell types to identify marker genes. The marker genes  
304 identified by COE should be more robust because they showed cell type-  
305 specificity across a broader range of cell types. This relationship will help to  
306 identify more brain cell marker genes from single-cell sequencing data, a  
307 technique that is increasing in popularity.

308 To explore the potential use of antibodies of NCM for cell labeling, we  
309 checked NCM's subcellular localization of expression in the COMPARTMENTS  
310 database<sup>35</sup> and the Allen Brain Atlas<sup>36</sup>. Eight human NCM and six mouse NCM  
311 are expressed on the plasma membrane, suggesting that antibodies made to  
312 these gene products have potential for use in FACS. One human NCM and  
313 seven mouse NCM are expressed at the nucleus, suggesting their potential use  
314 in sorting nuclei. Most of the mouse NCM already had archive ISH data except  
315 Elavl4. However, for the human brain, only SNTA1 had ISH data in the database.  
316 More experiments are needed to verify the subcellular location of the human  
317 NCM.

318 Supervised deconvolution was developed to replace the physical sorting of  
319 cell types. Supervised deconvolution infers cell proportion based on the  
320 expression of cell marker genes. Consequently, cell-type specificity of marker  
321 genes determines the accuracy of estimated proportions<sup>37</sup>. The deconvolution  
322 method is relatively well established, but validated marker genes for supervised  
323 deconvolution are lacking. NCM we proposed reduced the RMSE of  
324 deconvolution from 7.9% to 7.6% and resulted in improved accuracy of cell  
325 proportion estimates. The marginal improvement was expected because the  
326 baseline reference was composed of 400 genes with > 2-fold csFC. Instead of  
327 completing computations with 400 genes, using only the 21 GSM and 13 NCM  
328 we identified improved the performance of deconvolution slightly (0.3%) and is  
329 less resource intensive.

330 To date, various studies have found similarities and differences between  
331 tissue of humans and mice at the transcriptome level<sup>17,38-40</sup>. A study found a  
332 high degree of co-expression module preservation between human and mouse  
333 brain, and all mouse modules showed preservation with at least one human  
334 module whereas there were multiple human-specific modules<sup>41</sup>. The modules  
335 enriched in neuronal markers were more preserved between species than  
336 modules enriched glial marker genes<sup>41</sup>. This work conducted at the tissue level  
337 is consistent with our results showing that mouse shared BCCMs with human,  
338 but the BCCMs of the human brain were human-specific, except the neuron-  
339 related module. Our results also supported a recently published work at the  
340 single-cell level by Xu *et al.* who observed that hundreds of orthologous gene  
341 differences between human and rodent were cell type-specific<sup>42</sup>. Our data add  
342 to accumulating evidence that human have more cell-specific co-expression  
343 modules than mouse. Importantly, this implies that research on brain-related  
344 diseases using mouse models may have limited applicability to humans  
345 because of the difference between human and mouse brain cells. Furthermore,

346 the definitions of brain cell types should consider species differences.

347 Our work is limited by the lack of cell-specific gene expression data with a  
348 large sample size and replication. This made the criteria for the evaluation less  
349 universal and more specific to our data sets. We could only calculate the p-  
350 value for four of six DGEdats due to lack of replication. Another limitation is the  
351 data used in the discovery of the relationship between DGE and COE were not  
352 from the same samples. This may explain why we did not observe strong  
353 correlations in all tested datasets.

354 Through a comprehensive evaluation of the brain cell marker genes; we  
355 developed a new method to identify marker genes, and provide a list of reliable  
356 marker genes for brain cells to guide the cell identification. Recently, studies  
357 reported methylome<sup>43</sup> and regulome<sup>44</sup> of brain cells, creating the potential to  
358 develop marker genes at epigenetics level. It would be meaningful to construct  
359 a framework by combining different omics data and methods to fully describe  
360 the cell types in the brain.

361

## 362 **Materials and Methods**

### 363 **DGEdats pre-processing and quality control**

364 We collected six datasets for the DGE-based evaluation. 1) DGEDat1<sup>15</sup>: Cells  
365 were isolated from the human temporal lobe cortex by immunopanning. We  
366 downloaded the fragments per kilobase of transcript per million mapped reads  
367 (FPKM) matrix. Fetal samples and genes with FPKM<0.1 in more than one  
368 sample were removed. 2) DGEDat2<sup>14</sup>: Cells were isolated from mouse cerebral  
369 cortex by immunopanning and FAC. We downloaded the expression level  
370 estimation which was quantified as FPKM. Genes with FPKM<0.1 in more than  
371 two samples were removed. 3) DGEDat3<sup>10</sup>: Gene expression of cells isolated  
372 from mouse brain cortex were measured by microarray. The microarray data  
373 contained 12 cell populations, which made use of the Mouse430v2 Affymetrix  
374 platform. We downloaded the raw CEL file. All the CEL files were subjected  
375 together to background correction, normalization and summary value  
376 calculation using the R package affy<sup>45</sup> ('rma' function). The probes with 'A' or  
377 'M' state in more than two samples were removed. 4) DGEDat4<sup>11</sup>: Cells were  
378 isolated from E16.5 and P1 mouse brain to culture neuron and glia cells. We  
379 downloaded the expression matrix which were quantified as reads per kilobase  
380 of transcript per million mapped reads (RPKM). Genes with RPKM<0.1 in more  
381 than three samples were removed. 5) DGEDat5 and DGEDat6<sup>11</sup>: both primary  
382 cultured cells and acutely isolated cells were collected from four replicates of 9-  
383 week-old whole mouse brains. Liquid chromatography-tandem mass  
384 spectrometry analysis was performed. We downloaded the quantified  
385 expression matrix. Genes with one missing value were removed.

386

### 387 **COEdats pre-processing and quality control**

388 Two large-scale single-cell RNA sequencing datasets from both human and

389 mouse brain were collected for co-expression analysis. 1) COEDat1. The  
390 human single cell transcriptome was from adult human individual's temporal  
391 lobes<sup>46</sup>. In total, 332 cells from eight adult human brains (three males and five  
392 females) were collected and profiled by Illumina MiSeq and Illumina NextSeq  
393 500. Raw sequencing reads were aligned using STAR and per gene counts  
394 were calculated using HTSEQ. We downloaded the counts matrix. 2)  
395 COEDat2. The mouse single cell transcriptomes of 3005 cells from  
396 somatosensory cortex and hippocampal CA1 regions were collected from  
397 juvenile (P22 - P32) CD1 mice including 33 males and 34 females<sup>47</sup>. The  
398 sequencing platform was Illumina HiSeq 2000. Raw reads were mapped to the  
399 mouse genome using Bowtie and the mapped reads were quantified to raw  
400 counts. We downloaded the counts matrix.

401 COEDats were pre-processed in Automated Single-cell Analysis Pipeline  
402 (ASAP)<sup>48</sup>. Genes with Counts per Million (CPM) lower than 1 in more than ten  
403 samples were removed from human brain data, and genes with CPM lower than  
404 1 in more than 50 samples were removed from mouse brain data. After quality  
405 control, 13941 and 12149 genes were retained for human and mouse brain,  
406 respectively. The human brain data were normalized by voom function. Mouse  
407 data was normalized by scLVM. In total, 57 ERCC spike-ins in mouse data were  
408 used for fitting of technical noise. The normalized data were retained.

409

#### 410 **Deconvolution data pre-processing and quality control**

411 Gene expression data of brain samples with known cell proportion from rat  
412 was used in cell type-specific deconvolution<sup>31</sup> (GEO accession: GSE19380).  
413 This dataset contains four different cell types including neuron, astrocyte  
414 oligodendrocyte and microglia, and two replicates of five different mixing  
415 proportions (Supplementary Table 7). The platform used was Affymetrix Rat  
416 Genome 230 2.0 Array. All the CEL files were subjected together to background  
417 correction, normalization and summary value calculation using 'rma' function.

418

#### 419 **Co-expression analysis**

420 To determine the gene networks of specific cell types, we completed  
421 weighted gene co-expression network analysis (WGCNA<sup>22</sup>) on single-cell  
422 sequencing data from both human and mouse brain using the signed network  
423 type. The parameter settings were as follows: Pearson correlation function,  
424 signed Topological Overlap Matrix (TOM) matrix, minimal module size of 20,  
425 deepSplit of 4, mergeCutHeight of 0.25 and pamStage of true. The power for  
426 human and mouse data was 7 and 6, respectively. The number of modules for  
427 human and mouse data was 22 and 10, respectively. The pSI package was  
428 used to identify the cell-related modules. The threshold for the enrichment test  
429 was BH-corrected p-value<0.05. The GO terms analysis was identified by  
430 Gorilla<sup>49</sup>. The expression localizations of genes were provided by  
431 COMPARTMENTS<sup>35</sup>.

432

433 **Module preservation test**

434 A module preservation test was performed using the modulePreservation<sup>50</sup>  
435 function in the WGCNA R package. Zsummary is a measurement to assess the  
436 preservation based on the size, density and the connectivity of modules.  
437 Zsummary < 2 indicated the module was not preserved, 2 < Zsummary < 10  
438 indicated weak to moderate preservation, and Zsummary > 10 indicated high  
439 module preservation. We performed the module preservation test twice, once  
440 withmouse data as the reference and human data as the test set and once with  
441 roles reversed.

442

443 **Supervised deconvolution**

444 We used function 'lsmfit' in CellMix<sup>4</sup> for deconvolution. In each mixture sample,  
445 we tested i probes and j cell types. The expression of each probe equals the  
446 sum of expression of purified cell types times corresponding cell proportions:

447 
$$A_{11}X_1 + A_{12}X_2 + \dots + A_{1j}X_j = B_1$$

448 
$$A_{21}X_1 + A_{22}X_2 + \dots + A_{2j}X_j = B_2$$

449 
$$\dots \dots \dots$$

450 
$$A_{i1}X_1 + A_{i2}X_2 + \dots + A_{ij}X_j = B_i$$

451 Where  $A_{ij}$  is an expression signal of probe i in a purified cell j,  $B_i$  is an expression  
452 signal of probe i in a mixture of cells, and  $X_j$  is a proportion of cell type j. The  
453 formula can be summarized in a matrix equation:

454 
$$AX = B$$

455 where A is the reference matrix of the expression of all probe sets in all cell  
456 types, B is the vector of expression levels of all probe sets in the mixture, and  
457 X is the vector of the proportions of all cell types comprising B. The equation  
458 was solved for X with the R function 'lsmfit' (linear least squares algorithm).

459 The change of reference size was achieved by the following steps: 1)  
460 Construct the marker gene pool for four cell types and calculate the csFC. 2)  
461 Sort the marker gene pool according to the csFC in descending order. 3)  
462 Separate the reference genes into three types: GSM, NCM, and base genes.  
463 4) Pick the desired number of marker genes from the base gene pool to  
464 construct baseline reference and perform deconvolution. 5) Add the GSM,  
465 mouse\_NCM, or both GSM and NCM into the baseline reference to construct  
466 three tested references: gsm\_plus, ncm\_plus, gsm\_ncm\_plus. 6) perform  
467 deconvolution with three types of references separately. 7) Calculate RMSE  
468 between the estimated proportion and true proportion using the 'rmse' function  
469 in Metrics packages for each type of references. 9) Repeating step 2~step 8 for  
470 increasing reference sizes.

471 **Acknowledgments**

472 This work was supported by NSFC grants 81401114, 31571312, the National  
473 Key Plan for Scientific Research and Development of China  
474 (2016YFC1306000), and Innovation-Driven Project of Central South University  
475 (No. 2015CXS034, 2018CX033) (to C. Chen), and NIH grants 1U01

476 MH103340-01, 1R01ES024988 (to C. Liu). All the data contributors are  
477 sincerely thanked for the data provided. The authors thank Dr. Richard F. Kopp  
478 for critical reading of this manuscript.

## 479 **Author contributions**

480 R.D. designed the study, performed the analyses and wrote the paper. Y.C.,  
481 C.J., and J.D. helped with data collection and manuscript writing. C.L. and C.C  
482 created the project, supervised the study, contributed to the interpretation of the  
483 results, and revised the manuscript.

484

## 485 **Competing interests**

486 No competing interests declared.

487

## 488 **Reference**

- 489 1 Azevedo, F. A. *et al.* Equal numbers of neuronal and nonneuronal cells make the  
490 human brain an isometrically scaled-up primate brain. *The Journal of comparative  
491 neurology* **513**, 532-541, doi:10.1002/cne.21974 (2009).
- 492 2 Mancarci, B. O. *et al.* Cross-Laboratory Analysis of Brain Cell Type Transcriptomes with  
493 Applications to Interpretation of Bulk Tissue Data. *eNeuro* **4**,  
494 doi:10.1523/ENEURO.0212-17.2017 (2017).
- 495 3 Mullen, R. J., Buck, C. R. & Smith, A. M. NeuN, a neuronal specific nuclear protein in  
496 vertebrates. *Development* **116**, 201-211 (1992).
- 497 4 Gaujoux, R. & Seoighe, C. CellMix: a comprehensive toolbox for gene expression  
498 deconvolution. *Bioinformatics* **29**, 2211-2212, doi:10.1093/bioinformatics/btt351 (2013).
- 499 5 Newman, A. M. *et al.* Robust enumeration of cell subsets from tissue expression  
500 profiles. *Nature methods* **12**, 453-457, doi:10.1038/nmeth.3337 (2015).
- 501 6 Shen-Orr, S. S. & Gaujoux, R. Computational deconvolution: extracting cell type-  
502 specific information from heterogeneous samples. *Current opinion in immunology* **25**,  
503 571-578, doi:10.1016/j.coim.2013.09.015 (2013).
- 504 7 Fromer, M. *et al.* Gene expression elucidates functional impact of polygenic risk for  
505 schizophrenia. *Nature neuroscience* **19**, 1442-1453, doi:10.1038/nn.4399 (2016).
- 506 8 Yu, Q. & He, Z. Comprehensive investigation of temporal and autism-associated cell  
507 type composition-dependent and independent gene expression changes in human  
508 brains. *Scientific reports* **7**, 4121, doi:10.1038/s41598-017-04356-7 (2017).
- 509 9 Bachoo, R. M. *et al.* Molecular diversity of astrocytes with implications for neurological  
510 disorders. *Proceedings of the National Academy of Sciences of the United States of  
511 America* **101**, 8384-8389, doi:10.1073/pnas.0402140101 (2004).
- 512 10 Cahoy, J. D. *et al.* A transcriptome database for astrocytes, neurons, and  
513 oligodendrocytes: a new resource for understanding brain development and function.  
514 *The Journal of neuroscience : the official journal of the Society for Neuroscience* **28**,  
515 264-278, doi:10.1523/JNEUROSCI.4178-07.2008 (2008).
- 516 11 Sharma, K. *et al.* Cell type- and brain region-resolved mouse brain proteome. *Nature*

517 **neuroscience** **18**, 1819-1831, doi:10.1038/nn.4160 (2015).

518 12 Sugino, K. *et al.* Molecular taxonomy of major neuronal classes in the adult mouse  
519 forebrain. *Nature neuroscience* **9**, 99-107, doi:10.1038/nn1618 (2006).

520 13 Xu, X., Nehorai, A. & Dougherty, J. Cell Type Specific Analysis of Human Brain  
521 Transcriptome Data to Predict Alterations in Cellular Composition. *Syst Biomed (Austin)*  
522 **1**, 151-160, doi:10.4161/sysb.25630 (2013).

523 14 Zhang, Y. *et al.* An RNA-sequencing transcriptome and splicing database of glia,  
524 neurons, and vascular cells of the cerebral cortex. *The Journal of neuroscience : the  
525 official journal of the Society for Neuroscience* **34**, 11929-11947,  
526 doi:10.1523/JNEUROSCI.1860-14.2014 (2014).

527 15 Zhang, Y. *et al.* Purification and Characterization of Progenitor and Mature Human  
528 Astrocytes Reveals Transcriptional and Functional Differences with Mouse. *Neuron* **89**,  
529 37-53, doi:10.1016/j.neuron.2015.11.013 (2016).

530 16 Mouse Genome Sequencing, C. *et al.* Initial sequencing and comparative analysis of  
531 the mouse genome. *Nature* **420**, 520-562, doi:10.1038/nature01262 (2002).

532 17 Lin, S. *et al.* Comparison of the transcriptional landscapes between human and mouse  
533 tissues. *Proceedings of the National Academy of Sciences of the United States of  
534 America* **111**, 17224-17229, doi:10.1073/pnas.1413624111 (2014).

535 18 Januszyk, M. *et al.* Evaluating the Effect of Cell Culture on Gene Expression in Primary  
536 Tissue Samples Using Microfluidic-Based Single Cell Transcriptional Analysis.  
537 *Microarrays* **4**, 540-550, doi:10.3390/microarrays4040540 (2015).

538 19 Schwanhausser, B. *et al.* Corrigendum: Global quantification of mammalian gene  
539 expression control. *Nature* **495**, 126-127, doi:10.1038/nature11848 (2013).

540 20 Dong, X., You, Y. & Wu, J. Q. Building an RNA Sequencing Transcriptome of the Central  
541 Nervous System. *Neuroscientist* **22**, 579-592, doi:10.1177/1073858415610541 (2016).

542 21 Zhang, B. & Horvath, S. A general framework for weighted gene co-expression network  
543 analysis. *Statistical applications in genetics and molecular biology* **4**, Article17,  
544 doi:10.2202/1544-6115.1128 (2005).

545 22 Langfelder, P. & Horvath, S. WGCNA: an R package for weighted correlation network  
546 analysis. *BMC bioinformatics* **9**, 559, doi:10.1186/1471-2105-9-559 (2008).

547 23 Oldham, M. C. *et al.* Functional organization of the transcriptome in human brain.  
548 *Nature neuroscience* **11**, 1271-1282, doi:10.1038/nn.2207 (2008).

549 24 abcam. <<http://www.abcam.com/research/neuroscience/cell-type-marker>> (

550 25 MerckMillipore. <<http://www.merckmillipore.com/CN/zh/life-science-research/antibodies-assays/antibodies-overview/Research-Areas/neuroscience/Neurons-and-Glia/HtGb.qB.WxEAAFPBc51gPtr.nav>> (

551 26 Doyle, J. P. *et al.* Application of a translational profiling approach for the comparative  
552 analysis of CNS cell types. *Cell* **135**, 749-762, doi:10.1016/j.cell.2008.10.029 (2008).

553 27 Lein, E. S. *et al.* Genome-wide atlas of gene expression in the adult mouse brain.  
554 *Nature* **445**, 168-176, doi:10.1038/nature05453 (2007).

555 28 Hawrylycz, M. J. *et al.* An anatomically comprehensive atlas of the adult human brain  
556 transcriptome. *Nature* **489**, 391-399, doi:10.1038/nature11405 (2012).

557 29 Dugas, J. C., Tai, Y. C., Speed, T. P., Ngai, J. & Barres, B. A. Functional genomic  
558 analysis of oligodendrocyte differentiation. *The Journal of neuroscience : the official  
559 journal of the Society for Neuroscience* **34**, 11929-11947, doi:10.1523/JNEUROSCI.1860-14.2014 (2014).

561 journal of the Society for Neuroscience 26, 10967-10983,  
562 doi:10.1523/JNEUROSCI.2572-06.2006 (2006).

563 30 Dougherty, J. D., Schmidt, E. F., Nakajima, M. & Heintz, N. Analytical approaches to  
564 RNA profiling data for the identification of genes enriched in specific cells. *Nucleic acids*  
565 *research* **38**, 4218-4230, doi:10.1093/nar/gkq130 (2010).

566 31 Kuhn, A., Thu, D., Waldvogel, H. J., Faull, R. L. & Luthi-Carter, R. Population-specific  
567 expression analysis (PSEA) reveals molecular changes in diseased brain. *Nature*  
568 *methods* **8**, 945-947, doi:10.1038/nmeth.1710 (2011).

569 32 Boldog, E. et al. Transcriptomic and morphophysiological evidence for a specialized  
570 human cortical GABAergic cell type. *Nature neuroscience* **21**, 1185-1195,  
571 doi:10.1038/s41593-018-0205-2 (2018).

572 33 Eng, L. F., Ghirnikar, R. S. & Lee, Y. L. Glial fibrillary acidic protein: GFAP-thirty-one  
573 years (1969-2000). *Neurochemical research* **25**, 1439-1451 (2000).

574 34 Cardona, A. E., Huang, D., Sasse, M. E. & Ransohoff, R. M. Isolation of murine  
575 microglial cells for RNA analysis or flow cytometry. *Nature protocols* **1**, 1947-1951,  
576 doi:10.1038/nprot.2006.327 (2006).

577 35 Binder, J. X. et al. COMPARTMENTS: unification and visualization of protein  
578 subcellular localization evidence. *Database : the journal of biological databases and*  
579 *curation* **2014**, bau012, doi:10.1093/database/bau012 (2014).

580 36 Sunkin, S. M. et al. Allen Brain Atlas: an integrated spatio-temporal portal for exploring  
581 the central nervous system. *Nucleic acids research* **41**, D996-D1008,  
582 doi:10.1093/nar/gks1042 (2013).

583 37 Avila Cobos, F., Vandesompele, J., Mestdagh, P. & De Preter, K. Computational  
584 deconvolution of transcriptomics data from mixed cell populations. *Bioinformatics* **34**,  
585 1969-1979, doi:10.1093/bioinformatics/bty019 (2018).

586 38 Strand, A. D. et al. Conservation of regional gene expression in mouse and human  
587 brain. *PLoS genetics* **3**, e59, doi:10.1371/journal.pgen.0030059 (2007).

588 39 Zheng-Bradley, X., Rung, J., Parkinson, H. & Brazma, A. Large scale comparison of  
589 global gene expression patterns in human and mouse. *Genome biology* **11**, R124,  
590 doi:10.1186/gb-2010-11-12-r124 (2010).

591 40 Dowell, R. D. The similarity of gene expression between human and mouse tissues.  
592 *Genome biology* **12**, 101, doi:10.1186/gb-2011-12-1-101 (2011).

593 41 Miller, J. A., Horvath, S. & Geschwind, D. H. Divergence of human and mouse brain  
594 transcriptome highlights Alzheimer disease pathways. *Proceedings of the National*  
595 *Academy of Sciences of the United States of America* **107**, 12698-12703,  
596 doi:10.1073/pnas.0914257107 (2010).

597 42 Xu, X. et al. Species and cell-type properties of classically defined human and rodent  
598 neurons and glia. *eLife* **7**, doi:10.7554/eLife.37551 (2018).

599 43 Luo, C. et al. Single-cell methylomes identify neuronal subtypes and regulatory  
600 elements in mammalian cortex. *Science* **357**, 600-604, doi:10.1126/science.aan3351  
601 (2017).

602 44 Lake, B. B. et al. Integrative single-cell analysis of transcriptional and epigenetic states  
603 in the human adult brain. *Nature biotechnology* **36**, 70-80, doi:10.1038/nbt.4038 (2018).

604 45 Gautier, L., Cope, L., Bolstad, B. M. & Irizarry, R. A. affy--analysis of Affymetrix

605 GeneChip data at the probe level. *Bioinformatics* **20**, 307-315,  
606 doi:10.1093/bioinformatics/btg405 (2004).

607 46 Darmanis, S. *et al.* A survey of human brain transcriptome diversity at the single cell  
608 level. *Proceedings of the National Academy of Sciences of the United States of  
609 America* **112**, 7285-7290, doi:10.1073/pnas.1507125112 (2015).

610 47 Zeisel, A. *et al.* Brain structure. Cell types in the mouse cortex and hippocampus  
611 revealed by single-cell RNA-seq. *Science* **347**, 1138-1142,  
612 doi:10.1126/science.aaa1934 (2015).

613 48 Gardeux, V., David, F. P. A., Shakjofci, A., Schwalie, P. C. & Deplancke, B. ASAP: a  
614 web-based platform for the analysis and interactive visualization of single-cell RNA-seq  
615 data. *Bioinformatics* **33**, 3123-3125, doi:10.1093/bioinformatics/btx337 (2017).

616 49 Eden, E., Navon, R., Steinfeld, I., Lipson, D. & Yakhini, Z. GOrilla: a tool for discovery  
617 and visualization of enriched GO terms in ranked gene lists. *BMC bioinformatics* **10**,  
618 48, doi:10.1186/1471-2105-10-48 (2009).

619 50 Langfelder, P., Luo, R., Oldham, M. C. & Horvath, S. Is my network module preserved  
620 and reproducible? *PLoS computational biology* **7**, e1001057,  
621 doi:10.1371/journal.pcbi.1001057 (2011).

622

623

624

625

626

627

628

629

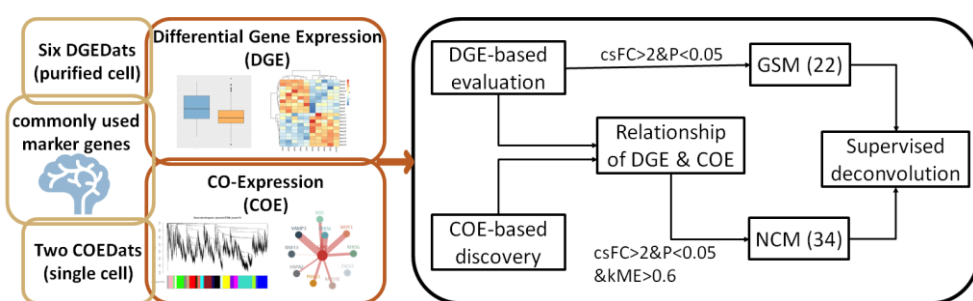
630

631

632

## 633 Figures and Tables

634



635

636 **Figure 1.** Analysis workflow. Six DGEDats of the purified cell population and two COEDats of single cells  
637 were used to evaluate 540 commonly-used brain cell marker genes. Differential gene expression (DGE)  
638 was performed on six DGEDats and the cell-specific fold change (csFC) was defined to measure the cell  
639 specificity for the marker genes. Co-expression (COE) analyses were performed on two COEDats and  
640 cell-specific networks were constructed. The correlation of genes with the module eigengene in the cell  
641 network was measured as module membership (kME). Through DGE-based evaluation, 22 gold-standard

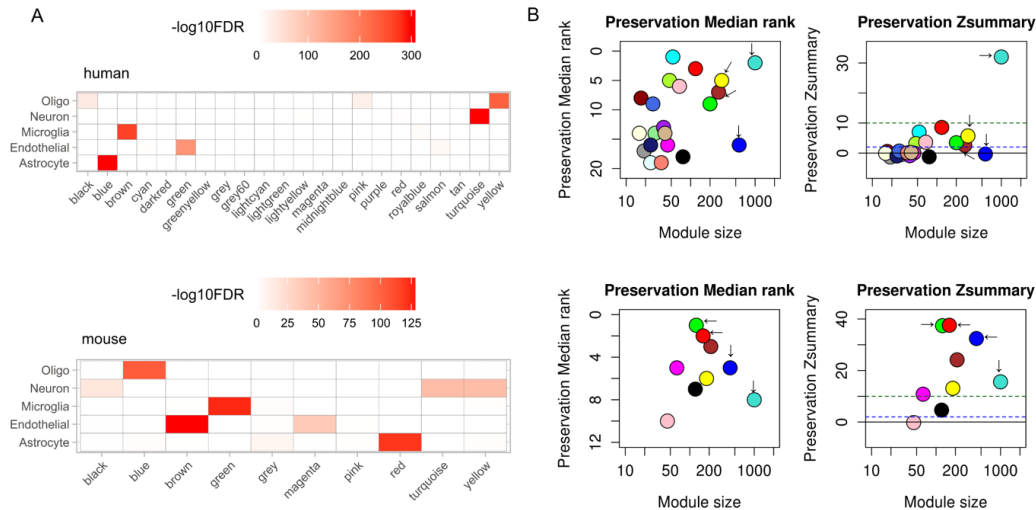
642 marker genes (GSM) were identified. Combining DGE and COE, 34 novel candidate marker genes (NCM)  
643 were identified. The specificities of GSM and NCM were demonstrated in supervised deconvolution.

644

645

646

647



648

649 **Figure 2.** Cell type enrichment and preservation test of co-expression modules for human and mouse  
650 brain. (A) Enrichment of brain cell marker genes in human and mouse co-expression modules. The most  
651 significantly enriched module was defined as the brain cell co-expression module (BCCM) for each cell  
652 type. The human BCCMs are blue (astrocyte), brown (microglia), turquoise (neuron), and yellow  
653 (oligodendrocyte). The mouse BCCMs are red (astrocyte), green (microglia), turquoise (neuron), blue  
654 (oligodendrocyte). (B) Preservation of BCCMs between human and mouse brain. The top panel is the  
655 preservation test of BCCMs of the human brain in mouse data. The bottom panel is the preservation test  
656 of BCCMs of the mouse brain in human data. The arrows point to the BCCMs.  $Z_{\text{summary}} < 2$  indicates  
657 the module is not preserved,  $2 < Z_{\text{summary}} < 10$  indicates weak to moderate preservation, and  $Z_{\text{summary}} >$   
658 10 indicates high module preservation.

659

660

661

662

663

664

665

666

667

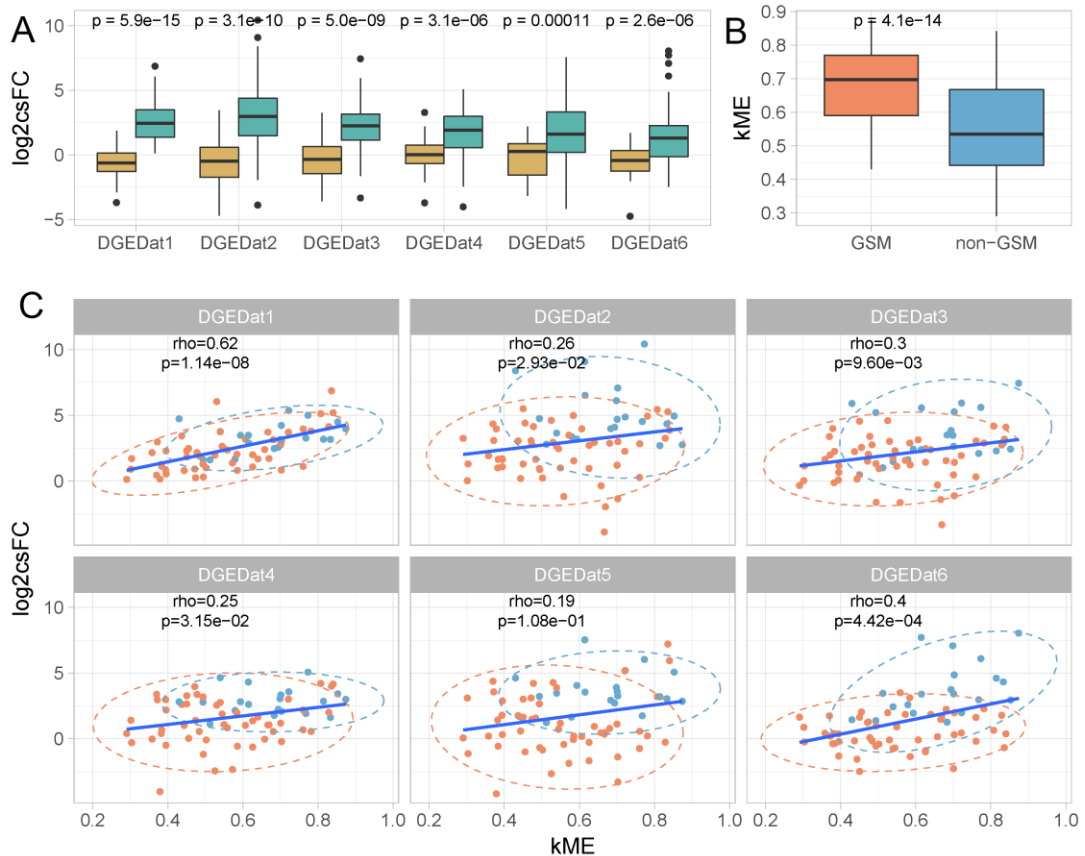
668

669

670

671

672



673

674 **Figure 3.** The relationship between DGE and COE of marker genes in human brains. (A) The comparison  
675 of csFC of BCCM marker genes and non-BCCM marker genes. The turquoise box denotes the marker  
676 genes in BCCMs and the mustard box denotes the marker genes in non-BCCMs ( $N_{\text{BCCM}} = 72$ ,  $N_{\text{NON-BCCM}}$   
677 = 35). The p-value is from a two-sample Wilcoxon test between csFC of marker genes in BCCMs and  
678 non-BCCMs. (B) The comparison of kME of the GSM and non-GSM in the BCCMs. A two-sample  
679 Wilcoxon test was used to test the significance of the difference ( $N_{\text{GSM}}=20$ ,  $N_{\text{non-GSM}}=52$ ). (C) The  
680 Spearman correlation between csFC and kME of marker genes in BCCMs. The blue dot represents GSM  
681 and the orange dot represent other marker genes. What are the dashed blue and orange circles?

682

683

684

685

686

687

688

689

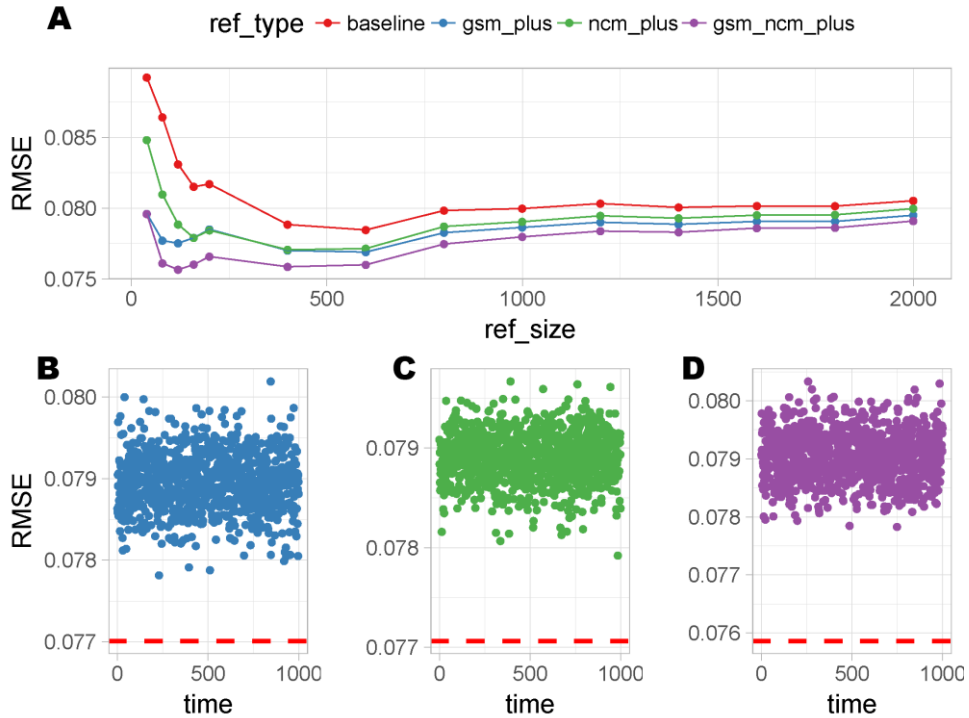
690

691

692

693

694



695

696 **Figure 4.** Effect of GSM and NCM in supervised deconvolution. (A) The RMSE between true and  
697 estimated cell proportion by supervised deconvolution with different references. The references are  
698 defined as follows: baseline = reference without GSM and mouse NCM; gsm\_plus = baseline + GSM;  
699 ncm\_plus = base + mouse NCM; gsm\_ncm\_plus = base + GSM +mouse NCM. With increasing size of  
700 the reference, the cell-specific fold change of marker genes included in the reference decreased. The  
701 deconvolution performance of permuted references without GSM and NCM where size is equal to the  
702 gsm\_plus (B), ncm\_plus (C), gsm\_ncm\_plus (D). The colors match the five references in figure 4A. The  
703 red dashed lines indicate the RMSE of deconvolution using gsm\_plus, ncm\_plus, and gsm\_ncm\_plus  
704 reference of 400 genes.

705

706

707

708

709

710

711

712

713

714

715

716

717

718

719

720

**Table 1** Datasets used

dataset	species	omics	platform	purification	Brain region	#sample/(cells)	study
DGEDat1	human	transcriptome	RNA-seq	isolated*	temporal lobe	45	GSE73721
DGEDat2	mouse	transcriptome	RNA-seq	isolated	cerebral cortex	17	GSE52564
DGEDat3	mouse	transcriptome	array	isolated	forebrain	10	GSE9566
DGEDat4	mouse	transcriptome	RNA-seq	culture*	Whole brain	22	Sharma et al.
DGEDat5	mouse	proteome	MS	culture	Whole brain	27	Sharma et al.
DGEDat6	mouse	proteome	MS	isolated	Whole brain	4	Sharma et al.
COEDat1	human	transcriptome	RNA-seq	isolated	somatosensory cortex and hippocampal CA1	(3005)	GSE60361
COEDat2	mouse	transcriptome	RNA-seq	isolated	temporal lobe	(332)	GSE67835

721

\*seq =RNA-sequencing, array = microarray, MS= mass spectrum, isolated= isolated from tissue, culture = primary culture. The table has to be shrunk to fit on a page and be within margin limits for the journal

722

723

724

725

726

727

728

729

730

731

732

733

734

735

736

737

738

739

740

741

742

**Table 2** csFC, standard deviation and p-value of GSM in differential expression analysis of six DGEDats

gene	cellType	DGEDat1	DGEDat2	DGEDat3	DGEDat4	DGEDat5	DGEDat6
PLP1*	oligo	<b>(5.01, 0.69, 1.63e-03)</b>	(10.43, 0.19, 1.67e-01)	(5.61, 0.44, 1.67e-01)	<b>(5.08, 0.47, 4.76e-05)</b>	(6.05, 0.79, 1.49e-06)	(6.11, NA, NA)
CNP	oligo	<b>(2.9, 0.42, 1.46e-03)</b>	(6.52, 0.48, 9.71e-02)	(5.58, 0.34, 1.04e-01)	<b>(2.63, 0.37, 8.01e-05)</b>	(3.56, 0.44, 3.77e-06)	(3.41, NA, NA)
SLC4A1	oligo	<b>(2.48, 0.26, 1.46e-03)</b>	(3.99, 0.33, 9.71e-02)	(3.51, 0.27, 1.04e-01)	<b>(1.8, 0.4, 8.01e-05)</b>	(2.94, 0.52, 1.39e-05)	(1.28, NA, NA)
MBP	oligo	<b>(3.49, 0.55, 1.46e-03)</b>	(9.09, 1.16, 9.71e-02)	(2.39, 1.18, 1.04e-01)	<b>(4.33, 0.51, 8.01e-05)</b>	(7.54, 0.67, 1.26e-04)	(7.72, NA, NA)
DCX	neuron	(1.64, NA, NA)	(4.76, 0.26, 9.71e-02)	(5.22, 0.32, 1.04e-01)	<b>(2.81, 0.31, 9.77e-05)</b>	(3.23, 0.79, 3.77e-06)	(1.4, NA, NA)
SLC12A5	neuron	(3.49, NA, NA)	(3.19, 0.44, 9.71e-02)	(2.42, 0.74, 1.04e-01)	<b>(2.83, 0.26, 9.77e-05)</b>	(4.07, 0.31, 3.77e-06)	(1.96, NA, NA)
GAD1	neuron	(5.38, NA, NA)	(4.87, 0.29, 9.71e-02)	(5.94, 0.36, 1.04e-01)	<b>(3.59, 0.42, 9.77e-05)</b>	(5.21, 0.51, 3.77e-06)	(2, NA, NA)
RELN	neuron	(4.74, NA, NA)	(8.4, 0.78, 9.71e-02)	(5.91, 0.32, 1.04e-01)	<b>(2.83, 0.23, 9.77e-05)</b>	(4.64, 0.46, 3.77e-06)	(1.46, NA, NA)
ITGAM*	microglia	<b>(3.16, 0.34, 1.91e-02)</b>	(6.12, 0.46, 1.25e-01)	(3.48, 0.78, 1.67e-01)	<b>(3.07, 0.2, 1.05e-02)</b>	(3.92, 0.54, 9.34e-04)	(7.09, NA, NA)
TLR7	microglia	<b>(2.88, 0.25, 2.11e-02)</b>	(5.64, 0.64, 9.71e-02)	(5.91, 0.29, 1.04e-01)	<b>(3.02, 0.14, 2.42e-03)</b>	(4.13, 0.52, 7.25e-04)	(6.32, NA, NA)
TLR2	microglia	<b>(4.24, 0.27, 2.29e-02)</b>	(7.09, 0.05, 9.71e-02)	(5.27, 0.2, 1.04e-01)	<b>(2.1, 0.23, 2.42e-03)</b>	(3.27, 0.73, 4.48e-05)	(4.87, NA, NA)
Alf1	microglia	<b>(2.81, 0.46, 2.29e-02)</b>	(5.16, 0.39, 9.71e-02)	(4.69, 0.4, 1.04e-01)	<b>(3.67, 0.36, 2.42e-03)</b>	(3.55, 0.68, 7.25e-04)	(4.89, NA, NA)
PTPRC	microglia	<b>(3.98, 0.24, 2.29e-02)</b>	(2.76, 0.62, 9.71e-02)	(7.44, 0.61, 1.04e-01)	<b>(3.01, 0.18, 2.42e-03)</b>	(2.87, 0.52, 4.48e-05)	(8.05, NA, NA)
GFAP*	astrocyte	<b>(3.19, 0.64, 5.76e-04)</b>	(2.7, 0.38, 5.00e-01)	(2.3, 0.54, 2.50e-01)	<b>(2.87, 0.37, 5.26e-03)</b>	(3.21, 0.51, 2.39e-03)	(4.62, NA, NA)
GJA1	astrocyte	<b>(4.5, 0.45, 1.81e-03)</b>	(4.96, 0.55, 9.71e-02)	(2.44, 0.48, 1.04e-01)	<b>(3.44, 0.26, 2.42e-03)</b>	<b>(5.08, 0.67, 1.58e-03)</b>	(2.96, NA, NA)
PPAP2B	astrocyte	<b>(3.28, 0.56, 3.63e-04)</b>	(4.53, 0.46, 9.71e-02)	(2.11, 0.41, 1.04e-01)	<b>(1.94, 0.29, 2.42e-03)</b>	(1.77, 0.53, 9.89e-03)	(2.98, NA, NA)
ALDH1L1	astrocyte	<b>(2.57, 0.3, 1.81e-03)</b>	(4.11, 0.32, 9.71e-02)	(3.85, 0.26, 1.04e-01)	<b>(2.26, 0.24, 2.42e-03)</b>	(2.73, 0.36, 9.89e-03)	(3.76, NA, NA)
SLC1A3	astrocyte	<b>(2.79, 0.34, 3.63e-04)</b>	(4.7, 0.46, 9.71e-02)	(2.65, 0.38, 1.04e-01)	<b>(3.34, 0.29, 2.42e-03)</b>	(3.6, 0.49, 9.89e-03)	(3.43, NA, NA)
SLC4A4	astrocyte	<b>(3.17, 0.38, 1.81e-03)</b>	(4.36, 0.61, 9.71e-02)	(2.9, 0.59, 1.04e-01)	<b>(1.63, 0.19, 2.42e-03)</b>	(3.06, 0.53, 1.58e-03)	(4.34, NA, NA)
CLU	astrocyte	<b>(3.77, 0.6, 3.63e-04)</b>	(3.65, 0.38, 9.71e-02)	(1.49, 0.34, 1.04e-01)	<b>(4.66, 0.24, 2.42e-03)</b>	(3.48, 0.44, 9.89e-03)	(2.45, NA, NA)
ALDOC	astrocyte	<b>(1.62, 0.68, 3.63e-04)</b>	(2.81, 0.37, 9.71e-02)	(1.02, 0.44, 1.04e-01)	<b>(1.14, 0.43, 2.42e-03)</b>	(1.25, 0.49, 3.02e-03)	(3.47, NA, NA)
NDRG2	astrocyte	<b>(1.68, 0.56, 3.63e-04)</b>	(3.4, 0.24, 9.71e-02)	(1.63, 0.22, 1.04e-01)	<b>(2.16, 0.19, 2.42e-03)</b>	<b>(1.66, 0.4, 1.58e-03)</b>	(2.6, NA, NA)

743 The numbers in the parentheses represent logarithmic transformed csFC, standard deviation and p-value of two-sample  
 744 Wilcoxon tests (log2csFC, SD, p-value); Bold numbers indicate the BH corrected p-value of two-sample Wilcoxon tests is  
 745 significant (FDR<0.05); oligo=oligodendrocyte; \*\* denotes this marker gene is a conflict marker gene. The neuron of DGEDat1

746 and all cell types in DGEDat6 have no replicates so statistical tests were not possible.

747

748

749

750

751

752

753

754

755

756

757

758

759

760

761

762

763

764

765

766

767

768

769

770

771

772

773

774

775

776

777

778

779

780

781

782

783

784

785

786

787

788

789

790 **Table 3** Brain cell co-expression modules in human and mouse

Species	module	# of genes	cellType	Top three hub genes	Gene ontology (q-value)
human	blue	731	astrocyte	AGXT2L1, GPR98, SLCO1C1	developmental process (3.85E-11)
human	brown	377	microglia	C3, ITGAX, LAPTM5	immune system process (1.00E-67)
human	turquois e	111 9	neuron	GABRB2, SNAP25, SYT1	regulation of trans-synaptic signaling (1.73E-19)
human	yellow	370	oligo*	UGT8, ERMN, OPALIN	axon ensheathment (2.39E-11)
mouse	red	187	astrocyte	GJA1, AQP4, NTSR2	multicellular organismal process (6.83E-08)
mouse	green	200	microglia	C1QA, C1QB, TYROBP	immune system process (8.79E-59)
mouse	turquois e	639 8	neuron	RAB3A, YWHAB, NDRG4	establishment of localization in cell (1.20E-35)
mouse	blue	475	oligo*	UGT8, CLDN11, CNP	axon ensheathment (7.85E-13)

791 \*oligo=oligodendrocyte; The 'top three hub genes' column displays the top three genes that have the highest kME within BCCM.

792 The 'gene ontology' column displays the top enriched category for each module.

793

794

795

796

797

798

799

800

801

802

803

804

805

806

807

808

809

810

811

812

813

814

815

816 **Table 4** NCM of human and mouse brain and their cellular locations

gene	cellType	species	ISH	location
ABCC9	oligodendrocyte	human	-	Plasma membrane
ACSS1	oligodendrocyte	human	-	Mitochondrial matrix
AHCYL1	oligodendrocyte	human	-	Cytoplasm
CXCR7	oligodendrocyte	human	-	Plasma membrane
DDAH1	oligodendrocyte	human	-	Cytosol
EMX2OS	oligodendrocyte	human	-	-
GNA14	oligodendrocyte	human	-	Plasma membrane
GPR125	oligodendrocyte	human	-	Plasma membrane
IL33	oligodendrocyte	human	-	Nucleoplasm
LRRC16A	oligodendrocyte	human	-	Plasma membrane
MT3	oligodendrocyte	human	-	Nucleus
PAPLN	oligodendrocyte	human	-	Extracellular region
RHOJ	oligodendrocyte	human	-	Plasma membrane
SLC14A1	oligodendrocyte	human	-	Plasma membrane
SNTA1	astrocyte	human	Y	Plasma membrane
TIMP3	astrocyte	human	-	Extracellular region
TPD52L1	astrocyte	human	-	Cytoplasm
WIF1	astrocyte	human	-	Extracellular region
C1qb	microglia	mouse	Y	Extracellular region
Mrc1	microglia	mouse	Y	Plasma membrane
Csf1r	microglia	mouse	Y	Plasma membrane
Ctss	microglia	mouse	Y	Lysosome
Ptpn6	microglia	mouse	Y	Nucleus
Cacna2d1	neuron	mouse	Y	Plasma membrane
Elavl4	neuron	mouse	-	Nucleus
SPin1	neuron	mouse	Y	Nucleus
Gria1	neuron	mouse	Y	Plasma membrane
Nipsnap1	neuron	mouse	Y	Mitochondrion
Slc25a22	neuron	mouse	Y	Plasma membrane
Mapk8	neuron	mouse	Y	Nucleus
Stau2	neuron	mouse	Y	Nucleus
Sirt2	oligodendrocyte	mouse	Y	Nucleus
Bcas1	oligodendrocyte	mouse	Y	Nucleus
Plxnb3	oligodendrocyte	mouse	Y	Plasma membrane

817 ISH: in situ hybridization image data from Allen Brain Atlas, Y: yes, having ISH image to confirm the locations, -: no ISH image.

818

819

820

821

822

823

824

825

826 **Supplementary Materials**

827 **Supplementary Figure 1.** The overlap of marker genes collected from different sources

828

829 **Supplementary Figure 2.** An example to illustrate the difference between cell-specific fold  
830 change and classic fold change

831 **Supplementary Figure 3.** The top 50 hub genes of human brain cell co-expression module

832 **Supplementary Figure 4.** The top 50 hub genes of mouse brain cell co-expression module

833 **Supplementary Figure 5.** The relationship between DGE and COE in co-expression  
834 analysis of mouse data

835 **Supplementary Figure 6.** Effect of human GSM in deconvoluting mouse brain tissue

836

837 **Supplementary Table 1.** Collected commonly-used brain cell marker gene

838 **Supplementary Table 2.** The classical fold change and cell type-specific fold change of  
839 consistent marker gene

840 **Supplementary Table 3.** The GO term of BCCM for human and mouse

841 **Supplementary Table 4.** NCM of mouse brain cell

842 **Supplementary Table 5.** NCM of human brain cell

843 **Supplementary Table 6.** DGE of RBFOX3 and TMEM119

844 **Supplementary Table 7.** The true proportion of cell types in the mixture for deconvolution

845

846

847

848

849

850

851

852

853

854

855

856

857

858

859

860

861

862

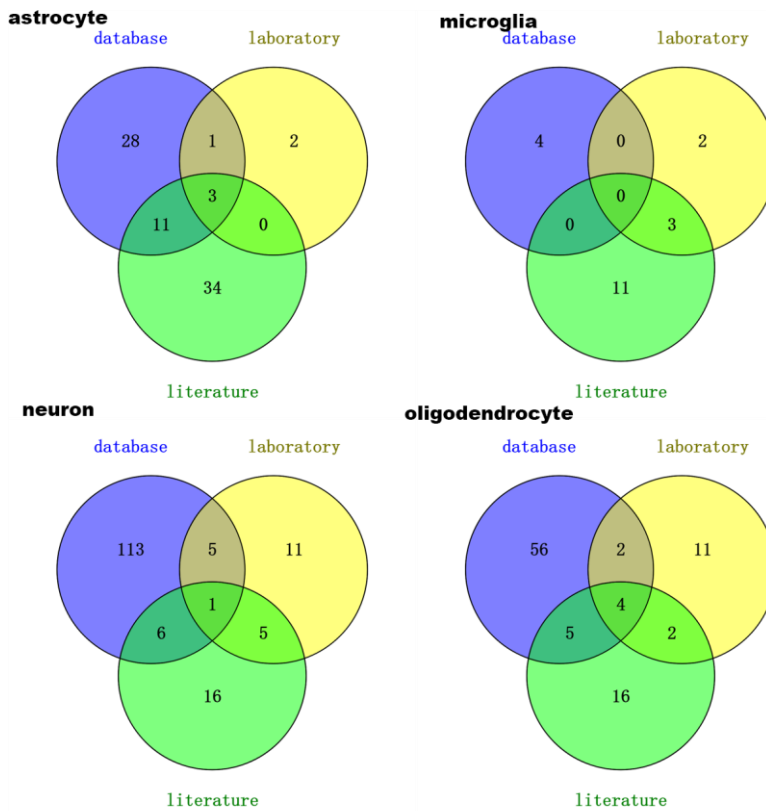
863

864

865

866

867



868

869 **Supplementary Figure 1** The overlap of marker genes collected from different sources. The commonly-  
870 used marker genes we evaluated were collected from three main sources: laboratory catalog, database,  
871 and published literature. The number indicates the number of marker genes belonging to corresponding  
872 sources.

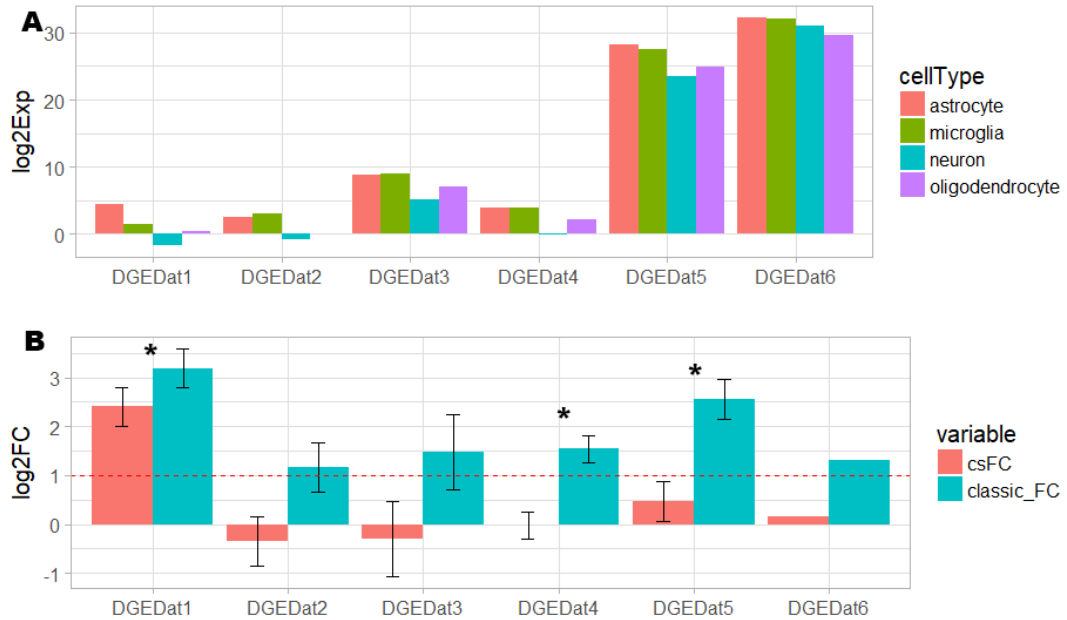
873

874

875

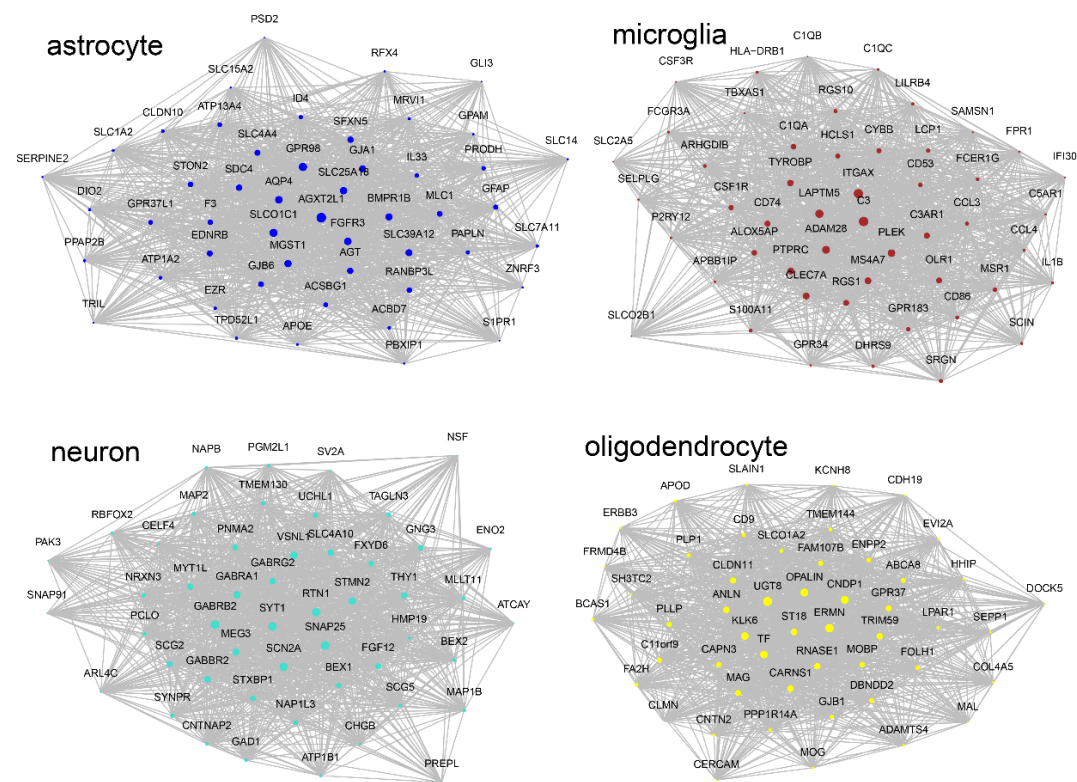
876

877



878  
879 **Supplementary Figure 2** An example to illustrate the difference between cell-specific fold change and  
880 classical fold change. (A) The expression of SELENBP1. SELENBP1 is an un-validated marker gene of  
881 astrocyte. All six DGEDats detected it. Its expression in microglia is very close to even higher than the  
882 expression in astrocyte in DGEDat2-DGEDat6. (B) The fold change of SELENBP1. The cell type-specific  
883 fold change (csFC) and classical fold change for the SELENBP1 are measured. The red dashed line is  
884 the empirical cut-off for the fold change ( $\log_2 FC = 1$ ). The error bar denotes the standard deviation of the  
885 fold change. The “\*” indicate the BH-corrected p-value of two-sample Wilcoxon test is lower than 0.05.  
886 Since DGEDat6 have no replicates, the standard deviation cannot be calculated. The similar expression  
887 in the microglia will be covered up by the classical fold change calculation, while the csFC avoids this  
888 situation.

889  
890  
891  
892  
893  
894  
895  
896  
897  
898  
899  
900  
901  
902  
903  
904  
905

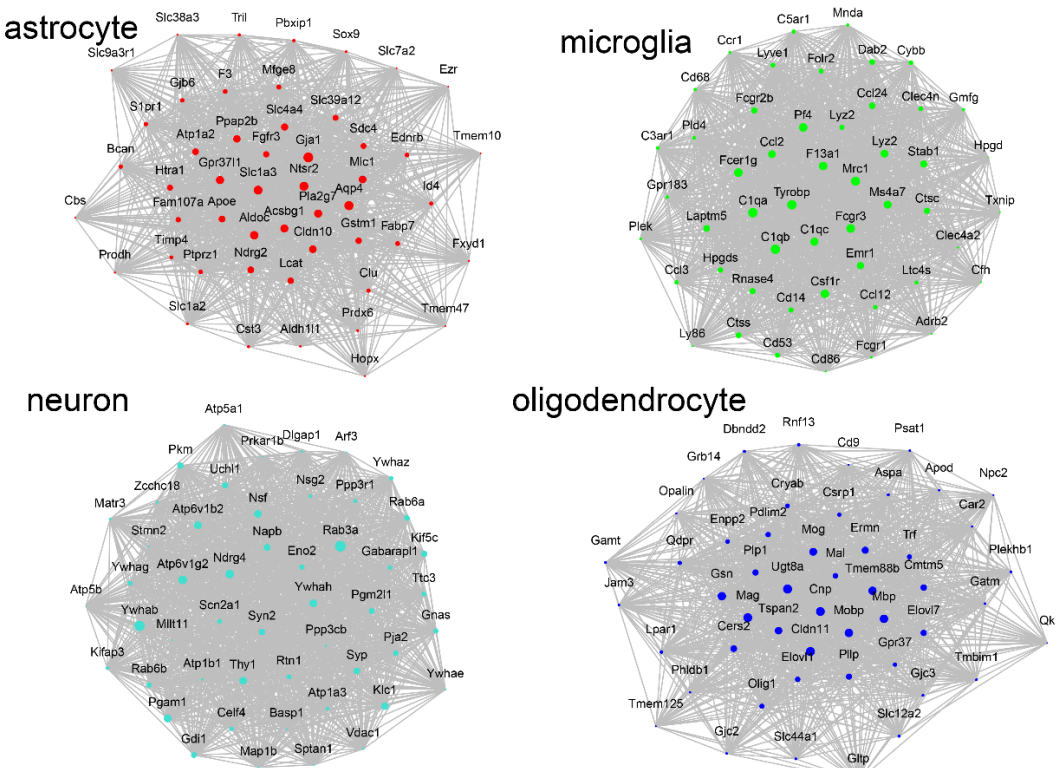


906

907 **Supplementary Figure 3** The top 50 hub genes of human brain cell co-expression module. The WGCNA  
908 was performed on human single-cell transcriptome. The brain cell co-expression module was selected  
909 according to the cell type enrichment conducted in pSI package. The gene members are ordered by kME  
910 from high to low. The dot color is the module color of brain cell co-expression module. The size of points  
911 indicates the kME of genes in the module with larger point representing higher kME.

912

913



914

915 **Supplementary Figure 4** The top 50 hub genes of mouse brain cell co-expression module. The WGCNA  
916 was performed on mouse single-cell transcriptome. The brain cell co-expression module was selected  
917 according to the cell type enrichment conducted in pSI package. The gene members are ordered by kME  
918 from high to low. The dot color is the module color of brain cell co-expression module. The size of points  
919 indicates the kME of genes in the module with larger point representing higher kME.

920

921

922

923

924

925

926

927

928

929

930

931

932

933

934

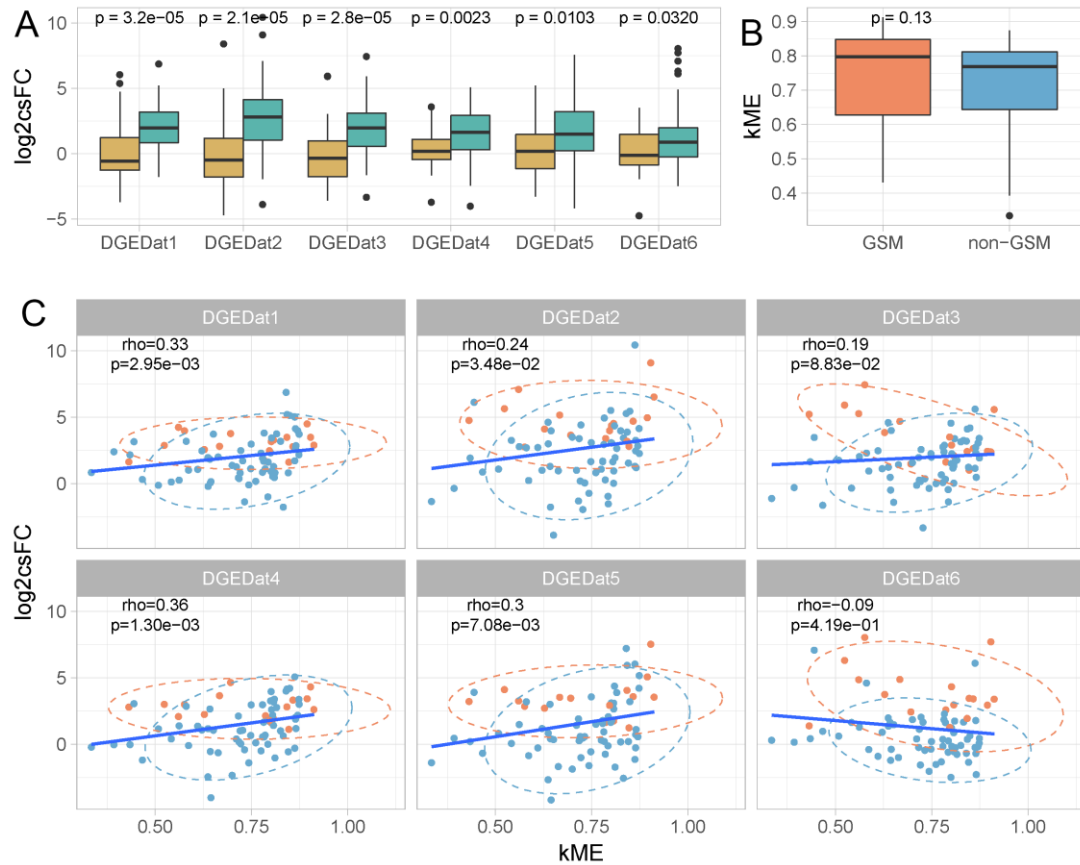
935

936

937

938

939



940

941 **Supplementary Figure 5** The relationship between DGE and COE in co-expression analysis of mouse  
942 data. (A) The comparison of csFC of brain cell co-expression module (BCCM) marker genes and non-  
943 BCCM marker genes. The turquoise box denotes the marker genes in BCCM and the mustard box  
944 denotes the marker genes in non-BCCM ( $N_{\text{BCCM}} = 79$ ,  $N_{\text{NON-BCCM}} = 28$ ). The p-value is from two-sample  
945 Wilcoxon test between csFC of marker genes in BCCMs and non-BCCMs. (B) The comparison of kME of  
946 the GSM and non-GSM in the BCCM. two-sample Wilcoxon test was used to test the significance of the  
947 difference ( $N_{\text{GSM}}=19$ ,  $N_{\text{non-GSM}}=88$ ). (C) The Spearman correlation between csFC and kME of marker  
948 genes in BCCMs. The blue dot represents GSM and the orange dot represent other marker genes.

949

950

951

952

953

954

955

956

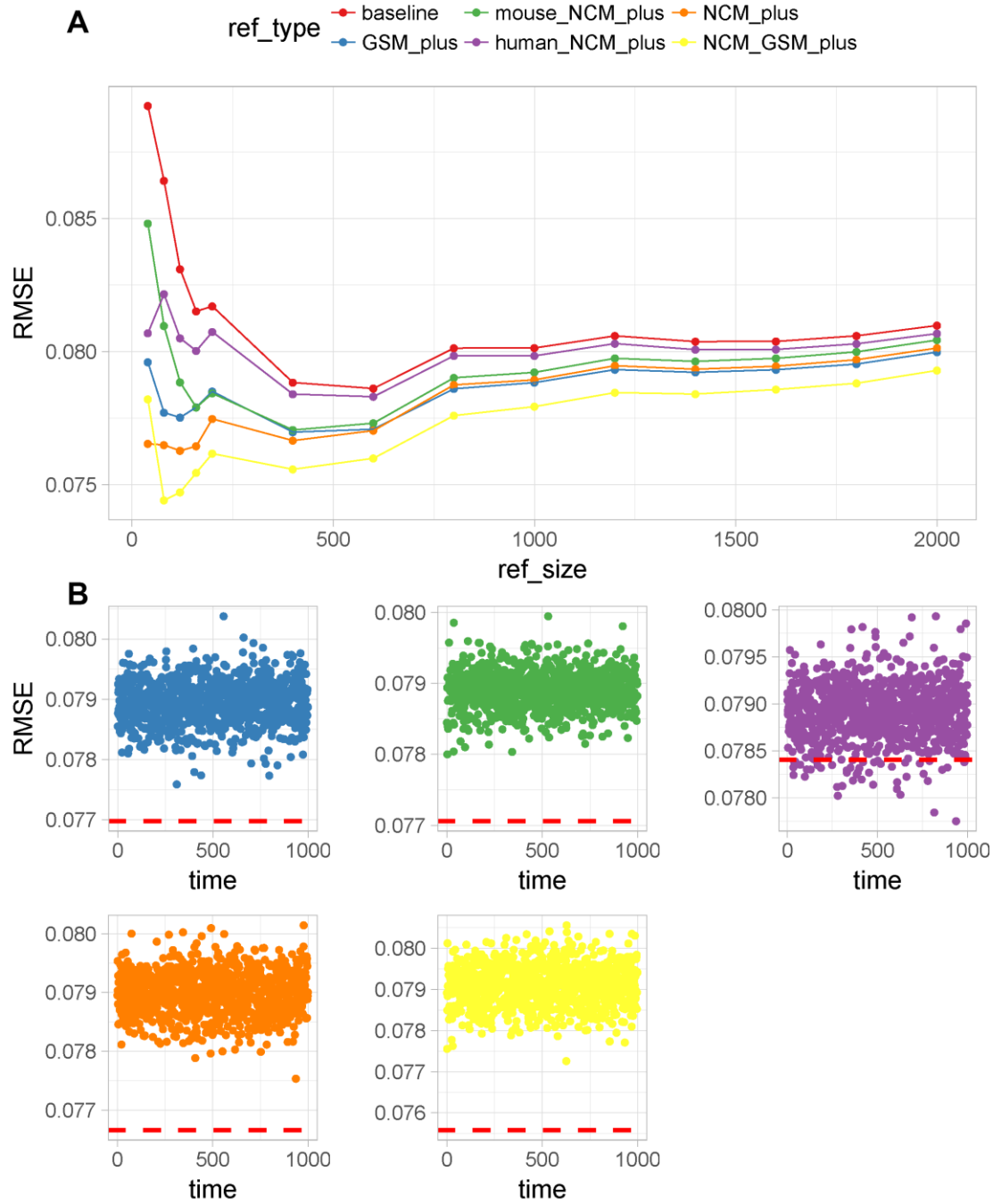
957

958

959

960

961



963 **Supplemental Figure 6** Effect of human GSM in deconvoluting mouse brain tissue. (A) The  
964 RMSE between true cell proportion and estimated cell proportion by supervised deconvolution  
965 with different references. The deconvolution performance of permuted references without  
966 GSM and NCM which size is equal to the reference tested above. The colors match the five  
967 references in figure 4A. The red dashed lines display the RMSE of deconvolution using tested  
968 reference of 400 genes.

969

970

971

972